The Geochemistry and Petrogenesis of Carnley Volcano, Auckland Islands, SW Pacific.

Journal:	*New Zealand Journal of Geology and Geophysics*
Manuscript ID	NZJG-2018-0036.R1
Manuscript Type:	Research Paper
Date Submitted by the Author:	19-Jul-2018
Complete List of Authors:	Gamble, John; Victoria University of Wellington, School of Geography, Environment and Earth Sciences; University College Cork, School of Biological, Earth and Environmental Sciences Adams, Chris; IGNS, GNS Science Morris, Paul; Geological Survey of Western Australia Wysoczanski, Richard; National Institute of Water and Atmospheric Research Handler, Monica; Victoria University of Wellington, School of Geography, Environment and Earth Sciences Timm, Christian; GNS Science Ltd
Keywords:	Intra-plate volcanism, Zealandia, SW Pacific, Auckland Islands, magma petrogenesis

The Geochemistry and Petrogenesis of Carnley Volcano, Auckland Islands, SW Pacific.

J.A. Gamble[a,b*], C.J. Adams[c], P.A. Morris[d], R.J. Wysoczanski[e], M. Handler[a], C. Timm[f]

[a]*School of Geography, Environment and Earth Sciences, Victoria University of Wellington, P.O. Box 600, Wellington, 6140, New Zealand;* [b]*School of Biological, Earth and Environmental Science, University College Cork, Ireland;* [c]*GNS Science, Private Bag 1930, Dunedin, New Zealand;* [d]*Department of Mines and Petroleum, Geological Survey of Western Australia, Perth, Western Australia;* [e]*National Institute for Water and Atmospheric Research, Private Bag 14901, Wellington, New Zealand;* [f] *GNS Science, PO Box 30-368, Lower Hutt 5040, Wellington, New Zealand.*

* Corresponding Author. E-mail: john.gamble@vuw.ac.nz

Editor: Gabor Kereszturi

Keywords: Intra-plate volcanism, Auckland Islands, Zealandia, S.W. Pacific, magma petrogenesis.

Abstract

Intraplate volcanism across Zealandia, South Eastern Australia, the Ross Sea Embayment and Marie Byrd Land in Antarctica define a magmatic province characterised by basalts with elevated $^{206}Pb/^{204}Pb$ (18.9 – 22.5), $^{87}Sr/^{86}Sr$ = ~0.7035, Light Rare Earth enrichment [$(Ce/Yb)_n$ > 10], and convex-up mantle normalised incompatible multi-element patterns, peaking at Nb-Ta, with negative K and Pb anomalies. Moreover, trace element abundances and ratios (e.g. Zr/Nb, Y/Zr) resemble those of Ocean Island Basalts (OIB), distinct from Mid-Ocean Ridge Basalt (MORB), suggesting derivation from distinctive (OIB-like) reservoirs. Our preferred scenario envisages partial melting across the garnet – spinel stability fields involving asthenospheric and lithospheric mantle components. This leads to an aggregated melting column where asthenospheric mantle is modelled by primitive mantle (PM) and subcontinental lithospheric mantle by depleted MORB mantle

(DMM) enriched by addition of 1% carbonatite (DMM+1). Melts accumulate in a column where the deep source is DMM and the shallower source a melange of DMM and subcontinental lithospheric mantle (DMM+1) across the lithosphere – asthenosphere boundary. Evolution of primary and near-primary magmas is controlled by olivine + clinopyroxene, then ol + cpx + plagioclase (pl) ± Fe-Ti oxides. The trachy-basalts, trachytes and rhyolites show isotopic evidence for interaction with continental crust.

Introduction

Auckland Islands (50.6°S, 166°E) are an archipelago of islands and sea stacks near the southern edge of the Campbell Plateau, ~ 400 km south of New Zealand, and form a part of the greater New Zealand lithospheric block of Zealandia (Luyendyk, 1995; Mortimer, 2008; Mortimer and Campbell, 2014). The islands (Figure 1) comprise the relics of two eroded Cenozoic intraplate shield volcanoes: Ross Volcano (Wright, 1966, 1967, 1968, 1970, 1971) in the north and Carnley Volcano (Speight and Finlayson, 1909, Gamble and Adams, 1985; Gamble et al., 1986; Gamble and Thomson, 1990) in the south that were active between 12 – 17 Ma before present (Adams, 1983; Hoernle et al., 2006). The rock types comprise a suite of mafic (basalt – trachy-basalt) lava flows that were erupted onto an eroded Mesozoic basement of biotite granite (Denison and Coombs, 1977) that is exposed on Musgrave Peninsula in the core of Carnley Harbour (Gamble and Adams, 1985). More evolved trachy-andesites, trachytes and rhyolites are present throughout the sequence, but are more common lower in the sequence and overall minor in volume. In this regard they are broadly similar, but with higher proportions of felsic lavas, to other subantarctic islands of the Campbell Plateau, namely Campbell Island (Morris, 1984; Gamble and Thomson, 1990), Antipodes Island (Gamble and Thomson, 1990; Scott et al., 2013) and the intra-plate volcanoes of the Chatham Rise and Southern New Zealand, (Morris, 1984, 1985; Baker et al., 1994; Weaver et al., 1989).

More recently, a number of researchers (Panter et al., 2000; 2006; 2018; Finn et al, 2005; Price et al., 2005; Hoernle et al., 2006; Sprung et al., 2007; Timm et al., 2009, 2010; McCoy-West et al., 2010, 2016; McGee et al., 2013; Kipf et al., 2013; Martin et al., 2013; Scott et al., 2013; 2014a, b; 2016a, b; Price et al, 2014; van Otterloo et al., 2014; van der Meer et al., 2017; Dalton et al, 2017) have addressed the regional trace element

and isotopic character of intra-plate basalts and their sources from southern Zealandia, the Ross Sea – West Antarctica margins of Antarctica and SE Australia that were once contiguous parts of the Gondwana margin prior to breakup ~ 105 - 85 Ma. A major debate has been the regional distribution of their distinctive geochemical characteristics with relatively low $^{87}Sr/^{86}Sr$, high $^{206}Pb/^{204}Pb$ and distinctive, convex-upward, mantle normalised multi-element incompatible trace element diagrams, with anomalies at K and Pb and described as HIMU-like (see Hoernle et al, 2006; Timm et al., 2009; 2010 McCoy-West et al., 2010 and Scott et al., 2013 for overviews). The debate focuses on whether these are melts sourced from a deep mantle plume, asthenospheric mantle, subcontinental mantle lithosphere or some combination of these sources.

Here we report the geochemistry of volcanic rocks and associated intrusions from Carnley Volcano in the Auckland Islands, including electron microprobe analyses of the major minerals, and whole rock major oxide, trace element and Sr, Nd and Pb isotope data. We evaluate the geochemical evolution of the magmas in the context of the volcanic stratigraphy and model the crystal fractionation and crustal assimilation pathways of the magmas as well as identifying primitive, near primary compositions that we use to interrogate possible source partial melting models in the context of the distinctive SW Pacific "HIMU-like" signature.

Establishing a regional geodynamic framework

A major thermal event ~ 180 Ma resulted from or led to the mantle instability that generated the massive continental flood basalt provinces of the Parana-Karroo-Ferrar, now preserved in Brazil, southern Africa, Antarctica, south eastern Australia and New Zealand and may have been a precursor to breakup of the Gondwana supercontinent and opening of the Tasman Sea and Southern Ocean, between 84 and 79 Ma (Gaina et al., 1998; Cande and Stock, 2004; van der Meer et al., 2017). Prior to these events and possibly since early Phanerozoic or late Proterozoic times, the continental lithosphere of the palaeo-Pacific margin had been subjected to subduction and subsequently to the possible effects of an impinging mantle plume. While mantle lithosphere, in its pristine form, is refractory and depleted in nature having been produced by partial melting processes that yielded basalt, this "lithospheric lid" may have been exposed periodically

to transitory melts and fluids that differentiate, mingle, degass and dewater, and variably infiltrate and enrich the lithospheric mantle. This is most certainly the case for the SW Pacific subduction-related margins of Gondwana and evidence of this process is recorded in mantle xenoliths from southern Zealandia (Scott et al., 2013; 2014a,b; 2016a,b; McCoy-West et al., 2015; 2016; Dalton et al, 2016), Antarctica (Gamble and Kyle, 1987; Gamble et al., 1988; Wysoczanski et al., 1993; Handler et al., 2003; Martin et al., 2014, 2015) and SE Australia (O'Reilly et al., 1988; Yaxley et al., 1991; McBride et al., 1996). The lithosphere of southern Zealandia comprises 20 – 30 km thick crust, coupled to lithospheric mantle whose thickness exceeds 100 km beneath the Southern Alps of New Zealand (Okaya et al., 2007; Davey et al., 2007) in broad agreement with estimations from mineral thermobarometry, (Scott et al., 2014a,b). For the purposes of this contribution, we assume an average crustal thickness of 20 - 25 km and lithospheric mantle thickness of 80 ± 10 km, approximating to ~ 2.5 ± 0.1GPa at the boundary with convecting mantle.

Geology of Carnley Volcano

The volcanic geology of Carnley Volcano is described in Gamble and Adams (1985) and Ritchie and Turnbull (1985). These papers describe the growth and development of Carnley basaltic shield volcano on the eroded Mesozoic basement of the Campbell Plateau. In the case of the Auckland Islands, basement comprises a ~ 95 Ma Cretaceous granitoid (Denison and Coombs, 1977; Adams, 1983; Pickett & Wasserburg, 1989; Adams et al., 2017), that is exposed on Musgrave Peninsula in the core of Carnley Harbour (Gamble and Adams, 1985). Here, it is intersected by an intense plexus of dikes and sills related to Neogene volcanism (c.f. Gamble and Adams, 1985, Figs 5 and 6). Early stages of volcanism were explosive and possibly subaqueous with fine ash and pillowed lavas abundant in the basal succession on Musgrave Peninsula which is intercalated with thin carbonate sedimentary deposits (Ritchie and Turnbull, 1985) whose fossil assemblages indicate late Oligocene – Miocene ages. Overlying lava flows and rarely preserved pyroclastic rocks are largely subaerial and individual lava flows and packages of flows can be traced over kilometre distances, with some flows up to 15 or 20 m thick. Potassium - Argon age dating of lava samples from Musgrave Peninsula are

reported in Adams (1983) and yield ages between 19 – 26 Ma in close agreement with the faunal assemblages. In the lower part of the succession, trachytes and rhyolites are more common than higher in the succession, where mafic rocks (basalts and trachy-basalts) are predominant. Nevertheless, the felsic rocks comprise < 5% of the volume exposed. The entire suite is intersected by a NNE-SSW trending dike swarm (Gamble and Adams, 1985, see Fig 4 for detailed map of Carnley Harbour region and Figs 5, 6, 10 and 12 for field photography) whose compositions span those of the lava flows. In the eroded interior of Carnley Harbour, on McClure Head and Circular Head, an intrusive complex of coarse grained, biotite-bearing, olivine gabbro and intimately associated minor felsic rocks (Gamble and Adams, 1985) has been emplaced into the base of the volcanic series. These rocks are genetically related to the overlying volcanic suite and appear to represent the cooled and crystallised contents of a shallow magma chamber.

Analytical Methods

Major and trace elements were determined by X-ray Fluorescence analysis in the Analytical Facility of Victoria University of Wellington on rock powders that were prepared by first chipping with an hydraulic splitter and then crushing to powder in a tungsten carbide grinding barrel. Major elements were determined on fused glass discs using this powder and following a modification of the method outlined by Norrish and Hutton, 1969. Standard United States Geological Survey and Geological Survey of Japan rocks were used for calibration and major oxides were determined to a precision of ± 1%. FeO was determined by standard titration protocols. Trace elements were determined on undiluted pressed rock powder discs supported by boric acid. Detection limits were of the order of 1-2 ppm for most elements and reproducibility (as determined by multiple runs on an internal laboratory standard) were better than ±5%. Scandium, Th, U and the rare earth elements (REE) were determined by Instrumental Neutron Activation Analysis (INAA) in the INAA Laboratory at New Mexico Institute of Mining and Technology, using strategies outlined in Gamble and Kyle (1987). Electron Microprobe analyses were made with a JEOL JXA-733 Superprobe in the Analytical Facility of Victoria University of Wellington fitted with three wavelength dispersive spectrometers. Measurements were calibrated against international standards and full ZAF correction protocols were used.

Standard minerals (e.g. PX-1) were regularly analysed during an analytical session as a monitor of instrumental drift and analytical precision. Analytical precision was generally better than 1% for oxides > 10% and between 5-10% for low concentration oxides.

All isotopes were measured on hand-picked rock chips (~ 5 mm across) that were first leached in an ultrasonic bath with dilute HCl, rinsed with distilled water and dried overnight at 60°C. Strontium and Neodymium isotopes were determined in the isotope facility of the Department of Geology, Royal Holloway University of London. Full details of the method used are in Thirlwall et al., (1994). During the time of the analyses SRM-987 gave $^{87}Sr/^{86}Sr = 0.710241 \pm 22$ (n=63) and La Jolla $^{143}Nd/^{144}Nd = 0.511857 \pm 7$ (n=17), with BCR-1 $^{143}Nd/^{144}Nd = 0.512621 \pm 5$ (n = 17). Lead isotopes were measured by RJW in the Department of Terrestrial Magnetism, Carnegie Institution, Washington. Lead isotope ratios were determined using a VG-P54 mass spectrometer with NIST-981 as an internal standard and correcting for mass fractionation using a $^{202}Pb/^{205}Pb$ double spike using methods outlined by Todt et al., 1996.

Petrology and Mineralogy

The rocks are variably porphyritic, containing up to 40% (volume) phenocrysts that comprise, in order of relative abundance, clinopyroxene, plagioclase, olivine and iron oxides. Olivine and clinopyroxene are more abundant in the mafic (basaltic) lavas, with plagioclase increasing in the intermediate (basaltic trachy-andesite) and felsic (trachytes and rhyolites) rocks where traces (~1- 2%) of sanidine are recorded. Olivine and clinopyroxene often occur as glomeroporphyritic aggregates showing evidence of variable resorption. Groundmass assemblages are plagioclase, clinopyroxene and iron oxides, with rare olivine, set in glass that is invariably altered. There is no evidence of a Ca-poor pyroxene. Composition ranges of representative olivine, clinopyroxene and plagioclase are summarised in Table 1, electron microprobe analyses are contained in the Supplementary Data.

Table 1 here

Olivine

Olivine compositions range from Fo_{86}–Fo_{51}, and no rocks contain olivine with compositions ~Fo_{90} that would be suggestive of near primary magma status. Typically phenocrysts show normal zoning, with Mg-rich cores and more Fe-rich rims (e.g. 82275, Fo_{86}- Fo_{56}; 82235, Fo_{84}- Fo_{67}). Groundmass olivine occurs in most rocks and compositions of these are typically Fe-rich, and similar to those of phenocryst rims.

Pyroxene

Clinopyroxene is ubiquitous as a phenocryst phase and in the groundmass of all the studied rocks. Phenocryst and groundmass compositions overlap with regard to Mg-content, but phenocrysts may show oscillatory compositional zoning and rare sector zoning, hinting at more complex petrological evolution.

Feldspar

Plagioclase occurs as a phenocryst and groundmass phase in all the rocks studied. Compositions range from An_{65} to An_{14}, with the less An-rich compositions representing groundmass and outer rims of phenocryst phases. In trachytes and rhyolites, rare sanidine occurs together with sodic plagioclase (~ An_{15}).

Fe-Ti oxides

Titano-magnetite and ilmenite occur as ubiquitous groundmass phases although there are sparse microphenocrysts of Ti-magnetite. Much of the Ti-magnetite shows textural evidence for subsolidus oxidation with lamellae of ilmenite.

Whole Rock Geochemistry

Major and Trace elements

Major and trace elements are shown for representative lava flows, dykes, sills and shallow intrusions in Table 2 and the entire data-base is lodged as Supplementary Data 2. Whole rock major oxide and trace element data are plotted in Figures 2 and 3. The Total Alkali versus Silica (TAS, Le Bas, 1986) diagram (Figure 2a) shows that most rocks are mafic and of basalt – trachy-basalt - basaltic trachy-andesite affinity. A composition gap

(54.5 – 62% SiO_2) separates the mafic samples from more evolved trachyte - rhyolite compositions. This bimodality is apparent in lava flows, dikes and sills and the shallow intrusions. When plotted in Harker-type diagrams (Figure 2 b – d) the trends of MgO, Al_2O_3, CaO and TiO_2 show variations that are also broadly consistent with magmatic evolution by fractional crystallisation.

Trace elements plots (Figure 3) of strongly incompatible elements define linear arrays among the basalts and trachy-basalts with ratios (e.g. Zr/Nb, Y/Zr, Ba/Zr) similar to those of OIB (5.8, 0.1, ~1.25 respectively, (Sun and McDonough, 1989) but distinct from MORB. More felsic rocks, such as the trachytes, rhyolites, and particularly, the felsic veins in the gabbro intrusions, deviate from the coherent trend of the basalts. In Figure 4, trace element ratios of Nb/Yb versus Th/Nb (Pearce, 2008) are plotted for selected primitive basalts from the Auckland Islands, together with representative samples from Banks Peninsula (Timm et al., 2009), Lookout Volcanics (McCoy-West et al., 2010), Antipodes Island (Scott et al., 2013) and Chatham Islands (Hoernle et al., 2006). The data fields overlap and fall in the Ocean Island Basalt (OIB) region of the OIB – MORB mantle array, confirming their OIB-like geochemical characteristics.

In Figure 5, chondrite normalised (Anders and Grevesse, 1989) REE are shown for a representative suite of samples. All rocks show light REE enriched patterns with (Ce/Yb) ranging from 8 – 15 and generally increasing with increasing SiO_2 content. Mafic rocks (e.g. #82235) show slight positive Eu-anomalies and evolved samples (e.g. #82254 and 82215) show distinct negative Eu-anomalies, the extent of the negative anomaly increasing with SiO_2 content.

Table 2 here

Primitive mantle normalised (Sun & McDonough, 1989) incompatible trace element abundances are shown as a series of multi-element plots in Figure 6. The mafic rocks (Figure 6a) show convex-up patterns typical of intraplate basaltic rocks with a maxima at Nb-Ta and a minor peak at U-Th, and with a relative depletion at K. The evolved rocks (Figure 6b) show peaks and troughs typical of felsic igneous rocks that have experienced significant degrees of crystal fractionation with peaks at Pb, and troughs at P (apatite), Ti

(Fe-Ti oxides), Sr and Ba (feldspar), consistent with extensive crystal fractionation and contamination by continental crust. The gabbro intrusion sample (#82285) shows a somewhat jagged pattern (Figure 6c), consistent with the cumulus nature of this rock. The felsic vein rock (#82289) shows a pattern similar to the evolved lavas of Figure 6b. Figure 6d compares multi-element patterns for primitive basalts across Zealandia, including the presently active Auckland Volcanic Field. Overall, the samples share many distinctive features, with convex-up patterns peaking at Nb-Ta, a K-anomaly and steep subparallel slopes to patterns for the less incompatible elements Nd-Lu.

Radiogenic isotopes

Radiogenic isotopes (Table 3) are plotted in conventional isotope variation diagrams (Figures 7 and 8). The Sr and Nd isotope results show the basalts occupying a restricted field, distinct from MORB (Figure 7). In detail however, the Auckland Islands suite define a curvilinear array extending between basalt and rhyolite at high values of $^{87}Sr/^{86}Sr$ and low values of $^{143}Nd/^{144}Nd$. Basaltic trachy-andesite and trachyte samples are intermediate between those of basalt and rhyolite. Basalts from other sub Antarctic Islands (Antipodes, Campbell and the Chatham Islands taken from Panter et al., (2006), Sprung et al., (2007), Hoernle et al., (2006), together with other data from southern New Zealand (Price et al., 2003; Timm et al., 2009, 2010) overlap with the Auckland Islands basalt data. The stippled area on Figure 7 shows the general field of New Zealand meta-sedimentary basement terranes of the Eastern and Western Provinces (data from Adams et al., 2005, Adams and Graham, 1996 and Price et al., 2015. Lead isotopes for basalts from the Auckland Islands (Figure 8 a,b) plot along the Northern Hemisphere Reference Line (NHRL) with $^{206}Pb/^{204}Pb$ varying between 19.5 and 20.0. Differentiated lavas (e.g. 82285, 82250) plot at lower $^{206}Pb/^{204}Pb$. Basalt data for other Zealandia intraplate sites (e.g. Campbell Island, Antipodes Island, Chatham Islands) extend to high $^{206}Pb/^{204}Pb \sim$ 20.6 and scatter about the NHRL. Nominal continental crustal values are proxied by GLOSS (Plank and Langmuir, 1998) and Average Upper Crust (UCC) (Rudnick and Gao, 2003) In plots of Sr- and Nd-isotopes versus $^{206}Pb/^{204}Pb$ (Figure 8c,d) the Auckland Island suite defines a curvilinear array between basalt and rhyolite consistent with magmatic evolution by assimilation with fractional crystallisation (AFC) processes.

Table 3 here

Discussion

Establishing P/T equilibria.

In Figure 9a we show results of calculations of P/T equilibration conditions for a suite of primitive basalts from the Auckland Islands (MgO > 9.0%, Ni > 200 ppm, Cr > 300 ppm). These are based on the thermo-barometric models of Wood (2004) and Lee et al., (2009). In the Wood (2004) calculations we use the whole rock compositions, recalculated to 100% anhydrous, with FeO as total iron. In the Lee et al., (2009) calculations, a preliminary step is the calculation of a primary magma by incremental addition of olivine until the melt reaches equilibrium with putative mantle olivine (here taken as Fo_{90}), and following Tamura et al (2000). On the P/T diagram, the mantle solidus is from Hirschman et al (2000), the liquidus from Katz et al (2003) and the plagioclase – spinel – garnet – stability fields are from Pearson et al (2005). The Lee et al. (2009) results yield pressures between 3.5 and 2.5 GPa and temperatures between 1550°C and 1500°C. The Wood (2004) determinations range between 2.5 GPa and 0.25 GPa and 1300° and 1250°C. The Lee et al., (2009) calculations result in higher pressure and temperatures because they calculate an initial primary magma in equilibrium with mantle olivine (Fo_{90}). Note how the data define 2 sub-parallel arrays, consistent with a polybaric fractionation pathway. Collectively, these results can be compared with the same data projected into the quaternary phase system C-M-A-S (O'Hara, 1968), Figure 9b, that shows data projected from olivine onto the plane CS-MS-A, with experimentally determined cotectics for 1GPa and one atmosphere. The Auckland Islands data cluster close to the plagioclase – clinopyroxene join at 1 GPa, consistent with phase equilibria involving fractionation of olivine + clinopyroxene + plagioclase. Primitive basalt compositions from Banks Peninsula (Timm et al., 2009) overlap with the Auckland Islands data set, suggesting broadly similar evolutionary pathways. Moreover, there is a degree of overlap in the P-T model presented here and the independently constrained xenolith model of Scott et al., 2014a.

Based on these observations, we suggest that the partial melting regime commenced in upwelling asthenospheric mantle beneath the trailing edge of the Zealandia lithospheric

plate. The melting column therefore commenced in the garnet stability field and moved upward into the spinel field in the shallower lithospheric mantle.

Quantification of crystal fractionation

Few, if any, of the analysed basalt samples in this study show geochemical features consistent with primary magmatic status (i.e. olivine >Fo_{90}, whole rock 100.Mg/Mg + Fe >70, high Ni and Cr), and we suggest that magmas have experienced varying degrees of crystal fractionation during ascent and that this is also allied to varying degrees of interaction with continental crust (AFC). To test this, we have performed stepwise least squares mixing calculations using iterations from primitive basalt to basalt, and from basalt to trachy-basalt and basaltic trachy-andesite, results of which are summarised in Table 4. Mineral data are from our database of electron microprobe analyses of minerals from the Auckland Islands. The least squares solutions show general agreement with the observed petrography with olivine (~Fo_{70-86}) + clinopyroxene ± plagioclase ± Fe-Ti oxides more dominant in the mafic rocks and clinopyroxene + plagioclase ± olivine ± Fe-Ti oxides in the more evolved (basaltic trachy-andesite) compositions. Steps to felsic compositions such as trachyte and rhyolite (e.g. #82254, Supplementary Table 3) show higher proportions of feldspar and essential involvement of Fe-Ti oxides and apatite. Using the mineral proportions from the least squares solutions and trace element partition coefficients from the Geochemical Earth Reference Model data base (GERM: EarthRef.org at http://earthref.org/), supplemented by values in Rollinson, (1998), we have used the Rayleigh equation to calculate normalised REE patterns for several evolutionary steps (e.g. basalt > trachy-basalt, basaltic trachy-andesite > trachyte). The basalt (82272) – trachy-basalt (82276) step is shown in Figure 10. Furthermore, the similarity of incompatible trace element ratios (Zr/Nb ~ 5, Y/Nb ~ 0.6, Ba/Zr ~ 1.25, Ba/Rb ~ 10, Figure 3) over much of the composition range hints at derivation from a common source, and magmatic evolution via broadly similar processes.

While fractional crystallisation offers a viable explanation for the overall within-suite variations, successive lava flows from measured sections (Figure 11) on Adams Island and the Fleming Plateau show irregular geochemical variations with stratigraphy, suggesting a more complex magmatic evolution, possibly sourced from spatially distinct

pockets or reservoirs at various depths beneath the volcano. Furthermore, radiogenic isotopic measurements imply interaction between ascending melts and shallow continental crust, which we examine in the following section.

Removing the veil of crustal contamination - Modelling Assimilation with Fractional Crystallisation (AFC).

The isotopic data show unambiguous evidence for interaction between mantle-derived magmas and continental crust during magmatic evolution, with rhyolites and trachytes (e.g. #82115) showing elevated $^{87}Sr/^{86}Sr$ and low $^{143}Nd/^{144}Nd$. In Figure 12, data for trachy-basalt, trachyte and rhyolite compositions define a curvilinear array towards higher $^{87}Sr/^{86}Sr$ and lower $^{143}Nd/^{144}Nd$, consistent with contamination by assimilation of continental crust. In Figure 12, we have modelled assimilation with fractional crystallisation (AFC) for Sr and Nd isotopes based on the algorithm of De Paolo, (1981). Our starting compositions were taken from the most primitive compositions from this work and supplemented by analyses from Panter et al., (2006); Hoernle et al., (2006); Sprung et al., (2007).

Selection of a crustal end-member contaminant is non-trivial. The middle to upper crust of the South Island, New Zealand is dominated by the juxtaposed Eastern and Western Province tectonostratigraphic terranes of relatively low-grade metamorphic rocks of the Torlesse, Rakaia and other Supergroups of the Eastern Province and Western terranes, exemplified by Buller Terrane, Greenland Group. They comprise packages of greywacke-type quartzo-feldspathic sandstones and associated argillites and typically show highly radiogenic Sr-isotope and unradiogenic Nd-isotope ratios. The Eastern and Western Provinces are separated by igneous rocks that comprise the Median Batholith (Mortimer et al., 1999). Paleogeographic reconstructions of van der Meer et al., (2017) indicate that Auckland Islands crust is of Western Province affinity although we note the presence of the Cretaceous age Musgrave granite in Carnley Harbour and metasedimentary rocks of Greenland Group affinity on Campbell Island (Adams et al., 2005). Our “shallow” crust contaminant is therefore defined by a composition based on a calculated average of the tectono-stratigraphic terranes estimated from the data-bases of Adams, (2005), Wandres et al., (2004) and Price et al., (2015).

Our modelling investigated a number of scenarios with fractionating mineral assemblages taken from our least squares models, partition coefficients were taken from the Geochemical Earth Reference Model data base (EarthRef.org at http://earthref.org/), and "r" values (where r = rate of assimilation/ rate of crystallisation) varied from 0.1 to 0.8. The best fit calculations were those in which r-values were > 0.6, suggesting relatively high input from mid-upper crustal rocks in the genesis of the evolved felsic rocks.

Modelling of partial melting

A number of recent papers (e.g. Finn et al., 2005; Panter et al., 2006; Sprung et al., 2007; Hoernle et al., 2006; Timm, 2009, 2010; McCoy-West et al., 2010, 2016; Scott et al., 2016, 2014a, b; Dalton et al., 2017) have addressed the matters of source versus process in the origin of the distinctive geochemical signatures of southern New Zealand continental intra plate basalts. In this regard, primitive basalts of the Auckland Islands carry the distinctive signature of HIMU-like mantle-derived basalts, with high U/Pb, light REE enrichment $(Ce/Yb)_n$ = 8 - 15, strongly convex upward multi-element patterns, peaking at Nb-Ta, and negative anomalies at K and Pb. Moreover, incompatible trace element ratios show characteristics of derivation from enriched OIB-like sources with Zr/Nb, Ba/Zr, Y/Zr, Rb/Zr similar to OIB, but distinctive from MORB (c.f. Figure 3).

There is considerable geochemical and petrological evidence from the study of mantle xenoliths from S.E. Australia (O'Reilly et al., 1988; Griffin et al., 1988; Yaxley et al., 1991; McBride et al., 1996), southern Zealandia (Scott et al., 2014, 2016a,b; McCoy-West et al., 2013, 2015, 2016, Liu et al., 2016; Dalton et al., 2017) and Antarctica (Gamble and Kyle, 1987; Handler et al., 2003; Martin et al, 2015; Panter et al, 2018) that the subcontinental lithospheric mantle is geochemically and mineralogically heterogeneous and has been variably metasomatised. Moreover, for Zealandia, Sm-Nd, Lu-Hf , U-Th-Pb and Re-Os model age calculations (McCoy-West et al. 2016; Scott et al. 2014, 2016b; Liu et al., 2015) have demonstrated depletion-enrichment events that extend from Palaeo-Proterozoic to late Phanerozoic times and have suggested mantle sources enriched by carbonatite as recently as 120 - ~100 Ma (Scott et al., 2014a,b; McCoy-West et al., 2016). Accordingly, for our modelling, we have selected Primitive Mantle (Sun &

McDonough, 1996, PM) for the convecting asthenospheric mantle source and depleted MORB mantle (Workman and Hart, 2010, DMM) enriched by addition of 1% calci-carbonatite (Hoernle, 2002) for lithospheric mantle (DMM+1%).

We have calculated aggregated partial melts using non-modal batch and fractional melting equations for selected trace elements, including REE, with residual garnet at high pressures and spinel at lower pressures, in keeping with a melting column traversing from garnet- to spinel-stability regions and from asthenospheric- to lithospheric-mantle. Partial melting through the asthenospheric mantle - lithospheric mantle boundary produces aggregated melts that show geochemical traces of both components (PM and DMM+1%) and agree with primitive melt compositions from Carnley Volcano. In our favoured model, partial melting commences in the asthenospheric mantle, modelled by PM in the garnet stability field and moves upward into shallower spinel-bearing metasomatised mantle in the lithosphere. The aggregated melts therefore carry signatures from both components. In Figure 13a, we show REE patterns for partial melts formed by small volume melting (~2%) of PM in the garnet stability field, followed by spinel or garnet melting of DMM+1%. The aggregated melts comprises a blend of 2% melt of asthenospheric mantle (PM) origin and up to 10% melt of lithospheric mantle (DMM+1) in the proportions 50:50 (Figure 13a) and 2% melt of asthenospheric mantle and 10% melt of lithospheric mantle (DMM+1), also with traces of residual amphibole, but in the proportions 70:30 (Figure 13b).

Lithospheric dimensions for the Campbell Plateau are reported by Davy et al., 2006, 2008; Grobys et al., 2008, 2009; Pysklywec et al., 2010; Ball et al., 2016. Significantly, Grobys et al., (2009) conclude that continental crust thins from around 33 km in the southern South Island, to 21 km beneath the Great South Basin, thickening again to ~27 km under the central Campbell Plateau. Moreover, three dimensional modelling by Pysklywec et al., 2010 suggest appreciable and abrupt thickness variations across the lithospheric mantle of southern Zealandia and this is further supported by results of the South Island Geophysical Transect (SIGHT) project (Davey et al., 2007; Okaya et al., 2007) that show thickened lithosphere to the SW of the South Island and fractures penetrating deep crust into lithospheric mantle. We therefore suggest that the lithosphere

– asthenosphere boundary beneath southern Zealandia is likely to be uneven and locally stepped.

In Figure 14, we present a cartoon model for the petrogenesis of the Auckland Islands basalts showing the trailing edge of the Zealandia Plate comprising continental crust and coupled lithospheric mantle moving westward at ~37mm yr^{-1} over asthenospheric mantle. In the absence of convincing structural, geophysical or tectonic evidence for impingment of any mantle plume body, and the apparent scattered distribution of volcanic centres and their age and duration in southern Zealandia, we are drawn to the concept of "edge-driven" convection of King and Anderson (1998). Using this theory, as developed by Demidjuk et al., (2007) for young intraplate volcanism in SE Australia, where a key parameter to establishing "edge driven" convective flow was identified as the existence of thickness variations (or "step" changes) at the lithosphere – asthenosphere boundary. We suggest that these necessary "steps" exist in southern Zealandia lithospheric mantle thickness and are suggested in the work of Grobys et al., 2009; Pysklywec et al., 2010 and Ball et al., 2016 with the boundary between lithosphere and asthenosphere likely to be locally irregular.

Motion of the southern Zealandia plate, coupled to the irregularity of the asthenosphere – lithosphere boundary, combines to establish conditions necessary for edge driven convective flow. Upwelling of asthenospheric mantle, thermo-mechanical erosion and entrainment of the lithospheric mantle into asthenospheric mantle produces conditions conducive to small volume partial melting and partial melts aggregate across a boundary that includes both lithospheric and asthenospheric mantle. Partial melts may be focussed and channelled via deep fractures or discontinuities similar to those identified in the SIGHT project. There is therefore no need for a mantle plume, the process is a consequence of plate tectonics.

Conclusions

Intraplate volcanism in Carnley Volcano results from partial melting along the trailing edge of the Zealandia lithospheric plate.

The primary melts are a result of polybaric decompression melting and melt aggregation across the garnet and spinel stability fields spanning asthenospheric and lithospheric mantle.

These primitive magmas evolve by fractional crystallisation and assimilation with fractional crystallisation (AFC) to form evolved felsic rocks such as rhyolite and trachyte. These rocks are minor in volume relative to the volumetrically dominant mafic melts and are concentrated lower in the stratigraphic succession, perhaps because in the early stages of volcanism, shallow (quartzo-feldspathic) crust was susceptible to partial melting and AFC by transiting mafic melts. As volcanism became established, melt channels became were lined by earlier melts and the ascending melts shielded from interaction with country rock.

Our preferred model favours a mechanism that is unrelated to a mantle plume, but in which the distinctive geochemical characteristics (e.g. OIB-like Zr/Nb, Y/Zr, Th/Yb, Nb/Yb, high Nb -Ta, low-K and HIMU-like Pb isotopes) are related to an edge-driven convective flow model (Demidjuk et al., 2007) in which convecting asthenospheric mantle and metasomatised lithospheric mantle interact to produce melts with OIB-like and HIMU-like characteristics. In this scenario, the lithospheric mantle carries the *HIMU-like* signature. This offers an explanation for the modern day geographic dispersion of geochemically similar intraplate magmas around the SW Pacific rim.

Acknowledgements

This paper began with the Department of Conservation coordinated expedition to the Auckland Islands during February – March 1982. JAG and CJA thank Ian Turnbull and Duncan Ritchie for companionship in the field at Carnley Harbour base-camp in Camp Cove.

Analytical work was undertaken in the Science Faculty Analytical Facility, VUW with assistance from Ken Palmer and Barry Roser. JAG thanks Royal Holloway University of London and Matthew Thirlwall and Martin Menzies for access to the radiogenic isotope laboratory and New Mexico Tech and Philip Kyle for access to INAA facilities. RW and MH thank Rick Carlson and Steve Shirey for access to the radiogenic laboratory at DTM.

Funding and logistic support from New Zealand Department of Conservation, Royal New Zealand Navy and Victoria University Internal Grants Fund was appreciated.
JAG thanks Martin Reyners, Rupert Sutherland, Donna Eberhard-Phillips, Bryan Davy, Nick Mortimer and Andy Tulloch for valuable advice and official manuscript reviews and comments and suggestions from Adam Martin and James Scott and Editor, Gabor Kereszturi that added critical content to the work.
Inspiration to complete this manuscript came from my co-authors and stimulating discussion with Adam Martin, James Scott, Chris Conway, Richard Price, Ian Smith, Joel Baker, Leo Pure and Colin Wilson.

References

Adams, C.J., 1983: Age of the volcanoes and the granite basement of the Auckland Islands, South West Pacific. New Zealand Journal of Geology and Geophysics, 26, 227 – 237.

Adams, C.J. and Graham, I.J., 1996: Metamorphic and tectonic geochronology of the Torlesse Terrane, Wellington, New Zealand. New Zealand Journal of Geology and Geophysics, 39 (2), 157 – 180.

Adams, C.J. and Kelley, S., 1998: Provenance of Permian – Triassic Ordovician meta-greywacke terranes in New Zealand: evidence from $^{40}Ar/^{39}Ar$ dating of detrital micas. Geological Society of America Bulletin, 110 (4), 422 – 432.

Adams, C.J. and Maas, R., 2004: Rb-Sr age and strontium isotope characteristics of the Greenland Group, Buller Terrane, New Zealand and correlations at the East Gondwanaland margin. New Zealand Journal of Geology and Geophysics, 47 (2) 189 – 200.

Adams, C.J., Pankhurst, R.J., Maas, R., Millar, I.L., 2005: Nd and Sr isotopic signatures of metasedimentary rocks around the South Pacific margin and implications for their provenance. In: *Vaughan, A.P.M, Leat, P.T., and Pankhurst, R.J. (eds) Terrane processes at the margins of Gondwana.* Geological Society of London, Special Publication, 246, 113 – 141.

Adams, C.J., Campbell, H.J., Mortimer, N., Griffin, W.L., 2017: Perspectives on Cretaceous Gondwana break-up from detrital zircon provenance of southern Zealandia sandstones. Geological Magazine, 154 (4), 661- 682.

Arevalo, R Jr. and McDonough, W.F., 2010: Chemical variations and regional diversity observed in MORB. Chemical Geology, 271, (1-2), 70 – 85.

Baker, J.A.; Gamble, J.A., Graham, I.J., 1994: The Age, Geology and Geochemistry of the Tapuaenuku Igneous Complex, Marlborough, New Zealand. New Zealand. Journal of Geology & Geophysics, v 37, 249 – 268.

Ball, J.S., Sheehan, A.F., Stachnik, J.C., Fan-Chi, L, Yeck, W.L., Collins, J.A., 2016: Lithospheric shear velocity structure of South Island, New Zealand, from amphibious Rayleigh wave tomography. Journal of Geophysical Research (Solid Earth), 121, 3686 – 3702.

Cande, S.C. and Stock, J.M., 2004: Cenozoic reconstructions of the Australia – New Zealand – South Pacific sector of Antarctica. In: The Cenozoic Southern Ocean: Tectonics, Sedimentation, and Climate Change between Australia and Antarctica 5 -17 (Eds. N.F. Exon, J.P. Kennett and M.J. Malone) American Geophysical Union, Washington, D.C. doi:10.1029/151GM02.

Cook, C., Briggs, R.M., Smith, I.E.M., Maas, R., 2005: Petrology and Geochemistry of Intraplate Basalts in the South Auckland Volcanic Field, New Zealand: Evidence for two coeval magma suites from distinct sources. Journal of Petrology, 46, no 3, 473 – 503.

Cooper, A.F. & Paterson, L.A. 2008: Carbonatites from a lamprophyric dyke swarm, South Westland, New Zealand. The Canadian Mineralogist, 46, 753 – 777.

Dalton, H.B., Scott, J.M., Liu, J., Waight, T.E., Pearson, D.G., Brenna, M., Le Roux, P., Palin, M., 2017: Diffusion-zoned pyroxenes in an isotopically heterogeneous mantle lithosphere beneath the Dunedin Volcanic Group, New Zealand, and their implications for intraplate alkaline magma sources. Lithosphere, 9, (3), 463 – 475.

Davey, F.J., Eberhart-Phillips, D., Kohler, M.D., Bannister, S., Caldwell, G., Henrys, S., Scherwath, M., Stern, T.A., van Avendonk, H., 2007: Geophysical Structure of the Southern Alps Orogen, South Island, New Zealand. Geophysical Monograph 175, 47 - 74, American Geophysical Union.

Davy, B., 2006: Bollons Seamount and early New Zealand – Antarctic seafloor spreading. Geochemistry, Geophysics, Geosystems, 7, Q06021, doi:10.1029/2005GC001191.

Davy, B. K., Hoernle, K., Werner, R., 2008: Hikurangi Plateau: General structure, rifted formation, and Gondwana subduction history. Geochemistry, Geophysics, Geosystems, 9, Q07004, doi:10.1029/2007GC1855.

Demidjuk, Z., Turner, S., Sandiford, M., George, R., Foden, J., Etheridge, M., 2007: U-series isotope and geodynamic constraints on mantle melting processes beneath the Newer Volcanic Province in South Australia. Earth and Planetary Science Letters, 261, 517 – 533.

Denison, R.E and Coombs, D.S., 1977: Radiometric ages fro some rocks from Snares and Auckland Islands, Campbell Plateau. Earth & Planetary Science Letters, 34, 23 – 29.

De Paolo, D.J., 1981: Trace element and isotopic effects of combined wall rock assimilation and fractional crystallization. Earth and Planetary Science Letters, 53, 189 – 202.

Finn, C.A., Mueller, R.D., Panter, K.S., 2005: A Cenozoic diffuse alkaline magmatic province (DAMP) in the southwest Pacific without rift or plume origin. Geochemistry, Geophysics, Geosystems, 6. Q02005, doi:10.1029/2004GC000723.

Gaina, C., Muller, D.R., Royer, J.Y, Stock, J., Hardebeck. J., Symonds, P, 1998: The tectonic history of the Tasman Sea: a puzzle with 13 pieces. Journal of Geophysical Research, Solid Earth, v 103, Issue B6, 12413 – 12433, DOI: 10.1029/98JB00386.

Gamble, J.A., Morris, P.A., Adams, C.J., 1986: the Geology, Petrology and Geochemistry of Cenozoic Volcanic Rocks from the Campbell Plateau and Chatham Rise. In: Smith, I.E.M., (ed) Cenozoic Volcanism in New Zealand, Bulletin, Royal Society of New Zealand, 23 344 – 365.

Gamble, J.A., and Adams, C.J., 1985: Volcanic Geology of Carnley Volcano, Auckland Islands. New Zealand Journal of Geology and Geophysics, v 28, 43-54.

Gamble J.A. and Kyle, P.A., 1987: The origins of glass and amphibole in spinel wehrlite xenoliths from Foster Crater, McMurdo Volcanic Group, Antarctica. Journal of Petrology, 28, 755 – 779.

Gamble, J.A., McGibbon, F., Kyle, P.R., Menzies, M.A., Kirsch, I. 1988: Metasomatised xenoliths from Foster Crater, Antarctica: Implications for Lithospheric Structure and Processes beneath the Transantarctic Mountain Front. Journal of Petrology, *Special Lithosphere Issue*, pp 109 – 138.

Gamble J.A. and Thomson J.W. 1989: Volcanic Geology of Scott Island, Balleny Islands and New Zealand sub Antarctic Islands. In: Le Masurier W.E. and Thomson J. (editors) Atlas of Volcanoes of Antarctica and the sub Antarctic Regions. American Geophysical Union, Monograph Series, Antarctic Research Series, v48, 464 - 481.

Griffin, W.L., O'Reilly, S.Y., Stabel, A., 1988: Mantle metasomatism beneath western Victoria, Australia: II. Metasomatic processes in Cr-diopside lherzolites and Al-augite pyroxenites. Geochimica et Cosmochimica Acta, 52, 449 – 459.

Grobys, J.W.G., Gohl, K., Eagles, G., 2008: Quantitative tectonic reconstructions of Zealandia based on crustal thickness estimates. Geochemistry, Geophysics, Geosystems, 9 (1), Q01005, doi:10.1029/2007GC001691.

Grobys, J.W.G., Gohl, K., Uenzelmann-Neben, G., Davy, B., Barker, D., 2009: Extensional and magmatic nature of the Campbell Plateau and Great South Basin from deep crustal studies. Tectonophysics, 472, 213 – 225.

Handler, M.R., Wysoczanski, R.J., Gamble, J.A., 2003: Proterozoic lithosphere in Marie Byrd Land, West Antarctica: Re-Os systematics of spinel peridotite xenoliths. Chemical Geology, 196, 131- 145.

Hart, S.R., 1984: A large-scale isotope anomaly in the Southern Hemisphere Mantle. Nature, 309, 753 -757.

Hirschmann, M.M., 2000: Mantle solidus: Experimental constraints and the effects of peridotite composition. Geochemistry, Geophysics, Geosystems, Volume 1, 2000GC000070.

Hoernle, K., White, J.D.L., Bogaard, P.V.D., Hauff, F., Coombs, D.S., Werner, R., Timm, C., Garbe –Schonberg, D., Reay, A., Cooper, A.F., 2006: Cenozoic Intraplate volcanism on New Zealand: Upwelling induced by lithospheric removal. Earth and Planetary Science Letters, 248, 335 – 352.

Hoernle, K., Tilton, G., Le Bas, M.J., Duggen, S., Garbe-Schonberg, D., 2002: Geochemistry of oceanic carbonatites compared with continental carbonatites: mantle recycling of oceanic carbonate. Contributions to Mineralogy and Petrology, 142, 520 – 542.

Katz, R.F., Spiegelman, M., Langmuir, C.H., 2003: A new parameterization of hydrous mantle melting. Geochemistry, Geophysics, Geosystems, 4, doi:10.1029/2002GC000433.

King, S.D. and Anderson, D.L. 1998: Edge-driven convection. Earth and Planetary Science Letters, 160, 289 – 296.

Kipf, A., Hauff, F., Werner, R., Gohl. K., Van den Bogaard, P., Hoernle, K., Maicher, A., Kugel, A. 2014: Seamounts off the West Antarctic Margin: A case for non-hotspot driven volcanism. Gondwana Research. 25 (4), 1660 – 1679.

Le Bas, M.J., Le Maitre, R., Streckeisen, A., Zannetin, B., 1986: A chemical classification of volcanic rocks based on the total alkali – silica diagram. Journal of Petrology,, 27, (3) 745 – 750.

Lee, C-T., Luffi, P., Plank, T., Dalton, H., Leeman, W.P., 2009: Constraints on the depths and temperatures of basaltic magma generation on Earth and other terrestrial planets using new thermobarometers for mafic magmas. Earth and Planetary Science Letters, 279, 20 – 33.

Liu, J, Scott, J.M, Martin, C.E., Pearson, D.G., 2015: The longevity of Archean mantle residues in the convecting upper mantle and their role in young continent formation. Earth and Planetary Science Letters, 424, 109 – 118.

Luyendyk, B., 1995: Hypothesis for Cretaceous Rifting of East Gondwana caused by Subducted Slab Capture. Geology, 23, 373 – 376.

Martin, A. P., Cooper, A. F., Price, R.C., 2013: Petrogenesis of Cenozoic, alkalic volcanic lineages at Mount Morning, West Antarctica and their entrained lithospheric mantle xenoliths: Lithospheric versus asthenospheric mantle sources. Geochimica et Cosmochimica Acta, 122, 127 – 152.

Martin, A.P., Cooper, A.F., Price, R.C., 2014: Increased mantle heat flow with on-going rifting of the West Antarctic rift system inferred from characterization of plagioclase peridotite in the shallow Antarctic mantle. Lithos, 190-191, 173 – 190.

Martin, A.P., Price, R.C., Cooper, A.F., McCammon, C.A., 2015: Petrogenesis of the Rifted Southern Victoria Land Lithospheric Mantle, Antarctica, Inferred from Petrography, Geochemistry, Thermobarometry and Oxybarometry of Peridotite and Pyroxenite Xenoliths from Mount Morning Eruptive Centre. Journal of Petrology, 56 (1), 193-226.

McBride, J.S., Lambert, D.D., Greig, A., Nicholls, I.A., 1996: Multistage evolution of Australian subcontinental mantle: Re-Os isotopic constraints from Victorian Mantle xenoliths. Geology, 24, 631 – 634.

McCoy-West, A., J., Baker, J.A., Faure, K., Wysoczanski, R.J., 2010: Petrogenesis and origins of Mid-Cretaceous continental intraplate volcanism in Marlborough, New Zealand: implications for the long-lived HIMU magmatic mega-province of the SW Pacific. Journal of Petrology, 51, 2003 – 2045.

McCoy-West, A., J., Bennett, V.C., Puchtel I.S., Walker, R.J., 2013: Extreme persistence of cratonic lithosphere in the southwest Pacific: Palaeoproterozoic Os isotope signatures in Zealandia. Geology, 41, no. 2, 231 – 234.

McCoy-West, A.J., Bennett, V.C., O'Neill, H., St C., Hermann, J., Puchtel, I.S., 2015: The Interplay between Melting, Refertilisation and Carbonatite Metasomatism in Off-Cratonic Lithospheric Mantle under Zealandia: and Integrated Major, Trace and Platinum Group Element Study. Journal of Petrology, 56, No 3, 563 – 604.

McCoy-West, A.J., Bennett, V.C., Amelin, Y., 2016: Rapid Cenozoic ingrowth of isotopic signatures simulating "HIMU" in ancient lithospheric mantle: Distinguishing source from process. Geochimica et Cosmochimica Acta, 187, 79 – 101.

McGee, L.E., Smith, I.E.M., Millet, M-A., Handley, H.K., Lindsay, J.M., 2013: Asthenospheric Control of Melting Processes in a Monogenetic Basaltic System: a Case

Study of the Auckland Volcanic Field, New Zealand. Journal of Petrology 54, 2125 – 2153.

Morris, P.A., 1984 Petrology of the Campbell Island Volcanics, south west Pacific Ocean. Journal of Volcanology and Geothermal Research, 21, 119 – 148.

Morris, P.A., 1985: Petrology of Late Cretaceous alkaline volcanic rocks from the Chatham Islands, New Zealand. New Zealand Journal of Geology and Geophysics, 28, 253 – 266.

Mortimer, N., Gans, P, Calvert, A., Walker, N., 1999: Geology and thermo-chronology of the east edge of the Median Batholith (Median Tectonic Zone): a new perspective on Permian and Cretaceous Crustal Growth in New Zealand. The Island Arc, 8 (3) 404 – 425.

Mortimer, N., 2008: Zealandia. Arizona Geological Society Digest, 22, p227 – 233.
Mortimer, N. and Campbell, H., 2014: Zealandia: Our Continent Revealed. Penguin, NZ, 271 pp.

O'Hara, M.J., 1968: The bearing of phase equilibria studies on the origin and evolution of basic and ultrabasic rocks. Earth Science Reviews, 4, 69 – 133.

O'Reilly, S.Y, Griffin, W.L., 1988: Mantle metasomatism beneath western Victoria, Australia: I. Metasomatic processes in Cr-diopside lherzolites. Geochimica et Cosmochimica Acta, 52, 433 – 447.

Okaya, D., Stern, T.A., Davey, F., Henrys, S., Cox, S., 2007: Continent-Continent Collision at the Pacific/Indo-Australian Plate Boundary: Background, Motivation and Principal Results. Geophysical Monograph 175, 1- 18, American Geophysical Union.

Panter, K.S., Kyle, P.R., Smellie, J.L., 1997: Petrogenesis of a trachyte-phonolite succession at Mount Sidley, Marie Byrd Land, Antarctica. Journal of Petrology, 38 (9), 1225 – 1253.

Panter, K.S., Hart, S.R., Kyle, P.R., Blusztajn, Wilch, T., 2000: geochemistry of late Cenozoic basalts from the Crary Mountains: characterization of mantle sources in Marie Byrd Land, Antarctica. Chemical Geology, 165, 215 – 241.

Panter, K. S., Blusztain, J., Hart, S.R., Kyle, P.R., Esser, R., McIntosh, W.C., 2006: The origin of HIMU in the SW Pacific: evidence from interplate volcanism in southern New Zealand and sub-Antarctic Islands. Journal of Petrology, 47, 1673 - 1704.

Panter, K., Castillo, P, Kraus, S., Deering, C., McIntosh, W., Valley, J. Kitajima, K., Kyle, P., Hart, S., Busztajn, J., 2018: Melt Origin across a Rifted Continental Margin: a case for subduction-related metasomatic agents in the Lithospheric sources of Alkaline

Basalt, NW Ross Sea, Antarctica. Journal of Petrology, https://doi-org.helicon.vuw.ac.nz/10.1093/petrology/egy036.

Pysklywec, R.N., Ellis, S.M., Gorman, A.R., 2010: Three-dimensional mantle lithosphere deformation at collisional plate boundaries: A subduction scissor across the South Island of New Zealand. Earth and Planetary Science Letters, 289, 334 – 346.

Pearson, D.G., Canil, D., Shirey, S.B., 2003: Mantle Samples Included in Volcanic Rocks: Xenoliths and Diamonds, pp 171 – 275. In *The Mantle and Core* (ed. R.W. Carlson) Vol. 2 *Treatise on Geochemistry* (Eds. H.D. Holland and K.K. Turekian) Elsevier-Pergamon, Oxford.

Pearce, J.A., 2008: Geochemical fingerprinting of oceanic basalts with applications to ophiolite classification and the search for Archean Oceanic Crust. Lithos, 100, (1) 14 – 48.

Pickett, D.A. and Wasserburg, G.J., 1989: Neodymium and Strontium isotopic characteristics of New Zealand granitoids and related rocks. Contributions to Mineralogy and Petrology, 103, 131 – 142.

Plank, T. and Langmuir, C.H., 1998: The chemical composition of subducting sediment and its consequences for crust and mantle. Chemical Geology, 145, 325 – 394.

Price, R.C., Cooper, A.F., Woodhead, J.D., Cartwright, I., 2003: Phonolitic diatremes in the Dunedin Volcano, South Island, New Zealand. Journal of Petrology, 44, 2053 – 2080.

Price, R. C., Nicholls, I.A., Day, A., 2014: Lithospheric influences on magma compositions of late Mesozoic and Cenozoic intraplate basalts (the Older Volcanics) of Victoria, south-eastern Australia. Lithos, 206-207, 179 – 200.

Ritchie, D.D. and Turnbull, I.M., 1985: Cenozoic sediments at Carnley Harbour, Auckland Islands, New Zealand Journal of Geology and Geophysics, v 28, 55 – xx.

Rudnick, R.L. and Fountain, D.M., 1995:Nature and composition of continental crust: A lower crustal perspective. Reviews in Geophysics, 33, 267 – 309.

Rudnick, R. L. & Gao, S., 2003: Composition of the Continental Crust. Treatise on Geochemistry, Volume 3. *Editor: Roberta L. Rudnick. ISBN 0-08-043751-6. Elsevier, 2003, pp 1-64.*

Scott, J.M., Turnbull, I.M., Auer, A., Palin, M., 2013: The sub-Antarctic Antipodes Volcano: A <0.5 Ma HIMU-like Surtseyan volcanic outpost on the edge of the Campbell Plateau. New Zealand Journal of Geology and Geophysics, 56, (3) 134 – 153.

Scott, J. M., 2014a: Ancient melt depletion overprinted by young carbonatitic metasomatism in the New Zealand lithospheric mantle. Contributions to Mineralogy and Petrology, 167, 1 – 17.

Scott, J.M, Waight, T.E., van der Meer, Q.H.A., Palin, J.M., Cooper, A.F., Munker, C., 2014b: Metasomatized ancient lithospheric mantle beneath the young Zealandia microcontinent and its role in HIMU-like intraplate magmatism. Geochemistry, Geophysics, Geosystems, 15 (9), 3477 – 3501, doi:10.1002/2014GC005300.

Scott, J.M, Liu, J., Pearson, D.G., Waight, T.E., 2016a: Mantle depletion and metasomatism recorded in orthopyroxene in highly depleted peridotites. Chemical Geology, 441, 280 – 291.

Scott, J.M, Brenna, M., Crase, J.A., Waight, T.E., van der Meer, Q., Cooper, A.F., Palin, J.M., Munker, C., 2016b: Peridotitic lithosphere metasomatized by volatile-bearing melts, and its association with intraplate alkaline HIMU-like magmatism. Journal of Petrology, 57, (10) 2053 – 2078.

Speight, R. and Finlayson, A.M., 1909: Physiography and geology of the Auckland, Bounty and Antipodes Islands. *In*: C. Chilton (ed.) *The subantarctic islands of New Zealand*, Section 2, 85 – 159.

Sprung, P., Schuth, S., Munker, C., Hoke, L., 2007: Intraplate volcanism in New Zealand: the role of fossil plume material and variable lithospheric properties. Contributions to Mineralogy and Petrology, 153, 669 – 687.

Sun, S-S. and McDonough, W.F., 1989: Chemical and isotopic systematics of oceanic basalts: implications for mantle composition and processes. In: Saunders, A.D. and Norry, M.J., (eds) *Magmatism in oceanic basins*. Geological Society of London, Special Publication, 42, 169 – 206.

Tamura, Y., Yuhara, M., Ishii, T., 2000: Primary arc basalts from Daisen Volcano, Japan: equilibrium fractionation versus disequilibrium fractionation during supercooling. Journal of Petrology, 41, 431 – 448.

Timm, C., Hoernle, K., Van den Bogaard, P., Bindeman, I., Weaver, S., 2009: Geochemical evolution of Intraplate volcanism at Banks Peninsula, New Zealand: Interaction between asthenospheric and lithospheric melts. Journal of Petrology, 50, 6, 989 – 1023.

Timm, C., Hoernle, K., Werner, R., Hauff, F., Bogaard, P. van den, White, J., Mortimer, N., Garbe-Schonberg, D. 2010: Temporal and geochemical evolution of the Cenozoic intraplate volcanism of Zealandia. Earth Science Reviews, 98, 38 – 64.

Van Otterloo, J., Raveggi, M., Cas, R.A.F., Maas, R., 2014: Polymagmatic activity at the monogenetic Mount Gambier volcanic complex in the Newer Volcanic Province, S.E. Australia. Journal of Petrology, 55 (7) 1317 – 1351.

Van der Meer, Q.H.A., Storey, M., Scott, J.M., Waight, T.E., 2016: Abrupt spatial and geochemical changes in lamprophyre magmatism related to Gondwana fragmentation prior, during and after opening of the Tasman Sea. Gondwana Research, 36, 142 – 156.

Van der Meer, Q.H.A., Waight, T.E., Scott, J.M., Munker, C., 2017: Variable sources for Cretaceous to recent HIMU and HIMU-like intraplate magmatism in New Zealand. Earth and Planetary Science Letters, 469, 27 – 41.

Wandres, A.M., Bradshaw, J.D., Weaver, S., Maas, R., Ireland, T., Eby, N., 2004: Provenance analysis using conglomerate clast lithologies: a case study from the Pahau Terrane of New Zealand. Sedimentary Geology, 167, 57 – 89.

Weaver, S.D. and Smith, I.E.M., 1989: New Zealand Intraplate volcanism. In: Johnson, R.W., Knutson, J. and Taylor, S.R., (Eds) Intraplate Volcanism in Eastern Australia and New Zealand. Cambridge University Press, pp 157 – 188.

Wood, B. J., 2004, Melting of Fertile Peridotite with variable amounts of H_2O. Geophysical Monograph 150, IUGG Volume 19, The State of the Planet: Frontiers and Challenges in Geophysics, 69 – 80.

Workman, R.K. and Hart, S.R., 2005: Major and trace element composition of depleted MORB mantle (DMM). Earth and Planetary Science Letters, 231, (1-2) 53 – 72.

Wright, J.B., 1966: Contributions to the volcanic succession and petrology and of the Auckland Islands, New Zealand. I West coast section through the Ross Volcano. Transactions of the Royal Society of New Zealand, Geology, 3, 215 – 229.

Wright, J.B., 1967: Contributions to the volcanic succession and petrology and of the Auckland Islands, New Zealand. II Upper part of the Ross Volcano. Transactions of the Royal Society of New Zealand, Geology, 5, 71 - 87.

Wright, J.B., 1968: Contributions to the volcanic succession and petrology and of the Auckland Islands, New Zealand. III Minor intrusives on the Ross Volcano. Transactions of the Royal Society of New Zealand, Geology, 6, 1 - 11.

Wright, J.B., 1970: Contributions to the volcanic succession and petrology and of the Auckland Islands, New Zealand. IV Chemical analyses from the lower half of Ross Volcano. Transactions of the Royal Society of New Zealand, Earth Sciences, 8, 109 - 115.

Wright, J.B., 1971: Contributions to the volcanic succession and petrology and of the Auckland Islands, New Zealand. IV Chemical analyses from the upper parts of Ross

Volcano, including minor intrusions. Journal of the Royal Society of New Zealand, 1, 175 - 183.

Yaxley, G.M., Crawford, A.J., Green, D.H., 1991: Evidence for carbonatite metasomatism in spinel peridotite xenoliths from western Victoria, Australia. Earth and Planetary Science Letters, 107, 305 – 317.

Zindler, A., and Hart, S.R., 1986: Chemical Geodynamics. Annual Reviews of Earth and Planetary Sciences, 14, 493 – 571.

Captions to Figures

Figure 1 Location map showing Auckland Islands with Carnley Volcano to south and Ross Volcano to north (modified from Gamble and Adams, 1985). The inset map shows the central area of Carnley Harbour, with Cretaceous granite basement on Musgrave Peninsula and a shallow gabbroic intrusion on Circular Head and McClure Head. Dykes of the NNE-SSW trending dyke swarm are stylized. K-Ar age data from Adams, 1983 are in boxes.

Figure 2 Major oxide variation diagrams (in weight %), including: (a) Total Alkali (Na_2O+K_2O) v SiO_2 (TAS, Le Bas et al, 1986) and (b) MgO v CaO/Al_2O_3 for lava flows, dikes and sills and shallow intrusions from Auckland Islands. Fractionation vectors are shown for olivine, clinopyroxene and Ca-plagioclase; fractionational crystallisation of a nominated phase produces a trend in the direction of the arrow. Note the strong coherence of the array for mafic rocks and the bimodality between the mafic suite and the felsic samples.

Figure 3 Selected trace element variation diagrams (in parts per million) for Carnley Volcano rocks. OIB and MORB values are from Sun and McDonough, 1989. Note the coherency of highly and moderately incompatible elements Zr, Nb, Y, Ba and Rb in the mafic rocks and the apparent decoupling (crustal assimilation?) in the felsic rocks.

Figure 4 Nb/Yb versus Th/Yb (Pearce, 2008) for intraplate basalts from Auckland Islands, with data from Banks Peninsula (Timm et al., 2010), Lookout Volcanics, Marlborough (McCoy-West et al., 2010), Chatham Islands (Panter et al., 2006) and Antipodes Island (Scott et al., 2013) for comparison. MORB values are from Arevalo and M^{c}Donough (2010), continental crust from Rudnick and Gao (R&G) (2003) and Rudnick and Fountain (R&F) (1995), GLOSS from Plank and Langmuir (1989).

Figure 5 Chondrite normalised (Anders and Gevresse, 1989) Rare Earth Element (REE) diagrams for basalt, trachy-basalt, trachyte and rhyolite from Carnley volcano. Note the enriched LREE patterns and the Eu-anomaly in the trachyte and rhyolite.

Figure 6 Mantle normalised (Sun and McDonough, 1989) multi-element plots of strongly and moderately incompatible trace elements for selected (a) basalts, (b) evolved rocks

and (c) shallow intrusives from the Auckland Islands. Figure 6(d) shows comparative plots for data from Zealandia, West Antarctica, Marie Byrd Land. All the data show a maximum convexity at Nb, Ta and a negative anomaly at K.

Figure 7 Combined strontium and neodymium isotope variation for the Auckland Islands suite. BSE is bulk silicate earth (Rollinson, 1993). Comparison with data from Chatham Islands, Campbell Island, Antipodes Island and Dunedin volcano (PCB samples), data from Panter et al, 2006; Hoernle et al., 2006 and Price et al, 2003. New Zealand Continental Crust (NZ) is a nominal "average" for quartzo-feldspathic metasediments from compilations by Price et al., 2015, Adams et al., 2005.

Figure 8 Lead isotope data from Auckland Islands rocks compared with data from other sub Antarctic islands and Dunedin volcano. Evolved trachy-basalt, trachyte and rhyolite samples from Auckland Islands are indicated in Figure 8a, c and d. Nominal averages for continental crust (GLOSS and UC) from Plank and Langmuir (1998) and Rudnick and Gao (2003) are shown. NHRL is the Northern Hemisphere Reference Line (Hart, 1984) HIMU and EM II are mantle reservoirs from Zindler and Hart (1986).

Figure 9 (**a)** P-T cross section of lithosphere and convecting upper mantle beneath Auckland Islands. Calculations based on selected high Mg (MgO > 9.0%) lavas from Auckland Islands using P/T calibrations of Wood (2004) and Lee et al. (2009). Mantle solidus from Hirschman, (2000) and liquidus from Katz et al., (2000). Stability fields of peridotite assemblages from Pearson et al (2003). Dashed arrows are adiabats for potential temperatures of 1500°C and 1400°C and are for reference. Note that the Lee et al., (2009) formulation, first calculates a "primary" magma by addition of olivine until the liquid is in equilibrium with olivine of Fo_{90}. The Wood (2004) model uses input whole rock data.

Figure 9(b) CMAS (O'Hara, 1968) olivine projection onto the plane CS-MS-A for Mg-rich (>9.0% MgO) basalts from Auckland islands. The experimentally determined stability fields and peritectic points for 1 atmosphere and 1 Gpa are shown. Note that all basalts plot in the cpx stability field at ~1Gpa in agreement with observed phenocryst assemblage of olivine + clinopyroxene ± plagioclase petrography. The dashed field includes selected primitive samples from Banks Peninsula (Timm et al., 2009) and the Lookout Volcanics (McCoy-West et al. 2010).

Figure 10. Modelled REE for crystal fractionation calculations, based on results from least squares modelling from basalt (82272) to trachy-basalt (82276).

Figure 11 Nb and TiO_2 measurements from two measured stratigraphic section of lava flows on Adams Island and the Fleming Plateau (see Fig 1). Note there is no clear chemical variation with height in the section, implying that there is no simple or continuous variation with time.

Figure 12 $^{87}Sr/^{86}Sr$ versus $^{143}Nd/^{144}Nd$ for Auckland Island lavas with calculated AFC curves (De Paolo, 1979) with ticks at 5% intervals, and where r is the ratio of the rate of assimilation to crystallisation.

Figure 13 Results of partial melting calculations for basalt (82272) for batch and fractional partial melting, with accumulated aggregated melts. Further details of the partial melting experiments are contained in the diagrams and in Supplementary Materials.

Figure 14. Cartoon cross section of Zealandia lithosphere in the context of "edge driven convection" (after King and Anderson, 1998; Demidjuk et al., 2007 and Price et al., 2014) showing location of intraplate volcanoes and thermo- mechanical erosion (stylised) of base of lithosphere into upwelling asthenospheric mantle leading to magmatism and focusing through deep cross-lithosphere fractures.

Table 1 Summary of compositions of major rock forming minerals in Auckland Islands, Carnley Volcano volcanic rocks. Mineral analyses are contained in Supplementary Data.

Sample	olivine	clinopyroxene	Plagioclase
30175 (82275)	Fo 86 - 56	Mg 90 - 73	An 65 - 22
30163 (82263)	Fo 74 - 26	Mg 76 - 67	An 58 - 50
30135 (82235)	Fo 84 - 67	Mg 82 - 74	An 56 - 51
30190 (82290)	Fo 54 - 52	Mg 70 - 66	An 59 - 46
30162 (82262)	Fo 68 - 61	Mg 76 - 73	An 59 - 52
30186 (82286)	Fo 72 - 60	Mg 83 - 77	An 78 - 50
30185 (82285)	Fo 66 - 61	Mg 77 - 75	An 80 - 56

Table 2 Chemical analyses of representative samples from Carnley Volcano, Auckland Islands. Note *Fe_2O_3 (italics)* is total iron determined by XRF; FeO and Fe_2O_3 were determined by titration. Trace elements in *italics* were determined by INAA. The entire Auckland Islands data set is contained in Supplementary Data.

VUW no.	**30135**	**30162**	**30164**	**30154**	**30172**	**30176**	**30115**	**30150**	**30185**	**30189**
Field no.	**82235**	**82262**	**82264**	**82254**	**82272**	**82276**	**82215**	**82250**	**82285**	**82289**
Occurrence	flow	flow	flow	flow	flow	flow	flow	sill	shallow intn	shallow intn
SiO2	46.34	45.85	46.36	66.23	48.93	52.73	72.06	68.86	46.26	64.72
TiO2	2.75	3.12	2.8	0.54	2.44	2.18	0.4	0.59	1.76	0.78
Al2O3	11.88	14.59	12.48	14.59	12.01	16.43	14.46	13.86	17.66	16.19
Fe2O3	3.18	3.43	4.02	1.6	3.72	4.34	1.38	2.15	2.62	1.72
FeO	8.99	9.4	8.39	4.52	7.99	5.5	0.28	2.53	5.69	1.96
*Fe2O3**	*13.17*	*13.88*	*13.34*	*6.62*	*12.6*	*10.45*	*1.69*	*4.96*	*8.94*	*3.9*
MnO	0.15	0.19	0.17	0.06	0.17	0.13	0.01	0.04	0.12	0.06
MgO	8.93	7.95	9.99	0.37	9.58	2.8	0.08	0.37	7.57	0.96
CaO	9.77	9.6	9.64	0.69	9.99	6.45	1.24	0.45	14.97	1.7
Na2O	2.78	2.74	2.67	3.08	2.4	3.59	3.87	3.94	1.8	4.46
K2O	0.8	1.04	0.85	5.12	1.21	2.53	5.09	4.83	0.35	5.91
P2O5	0.47	0.59	0.52	0.11	0.42	0.79	0.05	0.16	0.09	0.16
LOI	2.52	1.39	1.16	2.4	0.93	1.72	0.7	1.56	0.13	0.54
Total*	99.56	100.94	99.98	99.81	100.68	99.80	99.65	99.62	99.65	99.38
Sc	24	22	25	13	27	14	10	10	35	4
V	222	268	250	3	241	158	<2	12	232	26
Cr	305	222	410	2	490	9	<2	3	158	2
Ni	201	149	223	29	150	11	<2	4	91	11
Cu	64	65	74	4	41	14	2	<2	114	26
Zn	121	114	112	160	114	123	148	168	50	55
Ga	19	21	20	29	21	26	28	27	20	25
Rb	13	21	19	182	34	77	196	193	9	257
Sr	495	670	496	161	457	583	227	197	630	185
Y	29	33	26	59	32	43	64	63	14	45
Zr	183	229	175	631	232	392	590	577	93	645
Nb	42	61	44	105	48	74	106	104	17	75
Cs	*<0.1*	*0.1*	*0.05*	*1.43*	*0.25*	*0.98*	*3.18*	*0.5*	*0.14*	*3.51*
Ba	*206*	*322*	*244*	*766*	*276*	*513*	*754*	*764*	*89*	*512*
La	*23.8*	*35.5*	*25.3*	*84.4*	*35.3*	*56.9*	*113.6*	*82.7*	*8.72*	*76.1*
Ce	*50.4*	*72.8*	*50.3*	*180.1*	*71.6*	*120.3*	*237.4*	*170.7*	*18.3*	*157.6*

Nd	*24.4*	*40.8*	*37.4*	*78*	*36.9*	*58.5*	*108.2*	*76.7*	*13.2*	*62*
Sm	*6.5*	*7.64*	*5.88*	*15.25*	*7.47*	*11.42*	*18.78*	*14.09*	*2.84*	*9.92*
Eu	*2.13*	*2.4*	*2.039*	*3.338*	*2.169*	*3.15*	*3.61*	*2.995*	*1.092*	*1.992*
Tb	*0.96*	*1.01*	*0.81*	*2.04*	*0.98*	*1.5*	*2.42*	*2.08*	*0.38*	*1.3*
Yb	*1.78*	*1.83*	*1.52*	*4.81*	*2.15*	*3.28*	*4.19*	*5.04*	*0.77*	*3.58*
Lu	*0.25*	*0.27*	*0.206*	*0.732*	*0.303*	*0.46*	*0.582*	*0.761*	*0.102*	*0.54*
Hf	*4.7*	*5.3*	*4.11*	*16.58*	*5.41*	*9.4*	*15.86*	*14.9*	*2.44*	*17.76*
Ta	*2.4*	*3.5*	*2.49*	*6.18*	*2.67*	*4.09*	*6.43*	*6.16*	*1*	*5.16*
Th	*2.4*	*3.9*	*2.57*	*18.11*	*5.29*	*10.06*	*20.17*	*18.22*	*0.95*	*18.55*
U	*0.5*	*0.8*	*0.65*	*4.2*	*1.26*	*2.2*	*5*	*5.19*	*0.18*	*3.54*

Total* = analytical total based on Total Fe2O3*; FeO and Fe2O3 determined by titration, LOI = Loss on ignition at 1000°C

Trace elements in italics by instrumental Neutron Activation, all others by XRF.
Sample numbers are VUW 30xxx and field numbers 822xx.

Table 3 Sr, Nd and Pb isotopic data for representative samples from Carnley Volcano, Auckland Islands. Details of analytical methods are in text

VUW no	Field no	Sr	Rb	87Sr/86Sr		87Sr/86Sr(12Ma)	Nd	Sm	143Nd/144Nd		Pb	206Pb/204Pb
30135	82235	508	13	0.702965	±8	0.702953	24.4	6.49	0.512424	±2	2	19.535
30150	82250	197	193	0.708216	±8	0.707749	76.7	14.1	0.512594	±31	31	18.798
30158	82258	257	131	0.705856	±9	0.705613	85.5	15.3	0.512631	±17	17	18.81
30162	82262	698	21	0.70348	±10	0.703466	40.8	7.64	0.512893	±1	<2	19.62
30162-r	82262-r										<2	19.622
30163	82263	640	21	0.703539	±9	0.703523	38.8	8.61	0.512905	±3	3	19.499
30164	82264	496	19	0.703593	±7	0.703575	37.4	5.88	0.512893	±1	<2	19.465
30172	82272	457	34	0.704303	±6	0.704267	36.9	7.47	0.512761	±2	2	19.067
30177	82277	536	16	0.703261	±8	0.703247	18.1	7.31	0.512894	±1	<2	19.883
30185	82285	630	9	0.703298	±8	0.703291	13.2	2.84	0.512865	±1	<2	19.716
30115	82215	227	196	0.709296	±8	0.708884	108.2	18.78	0.512562	±25	25	18.798

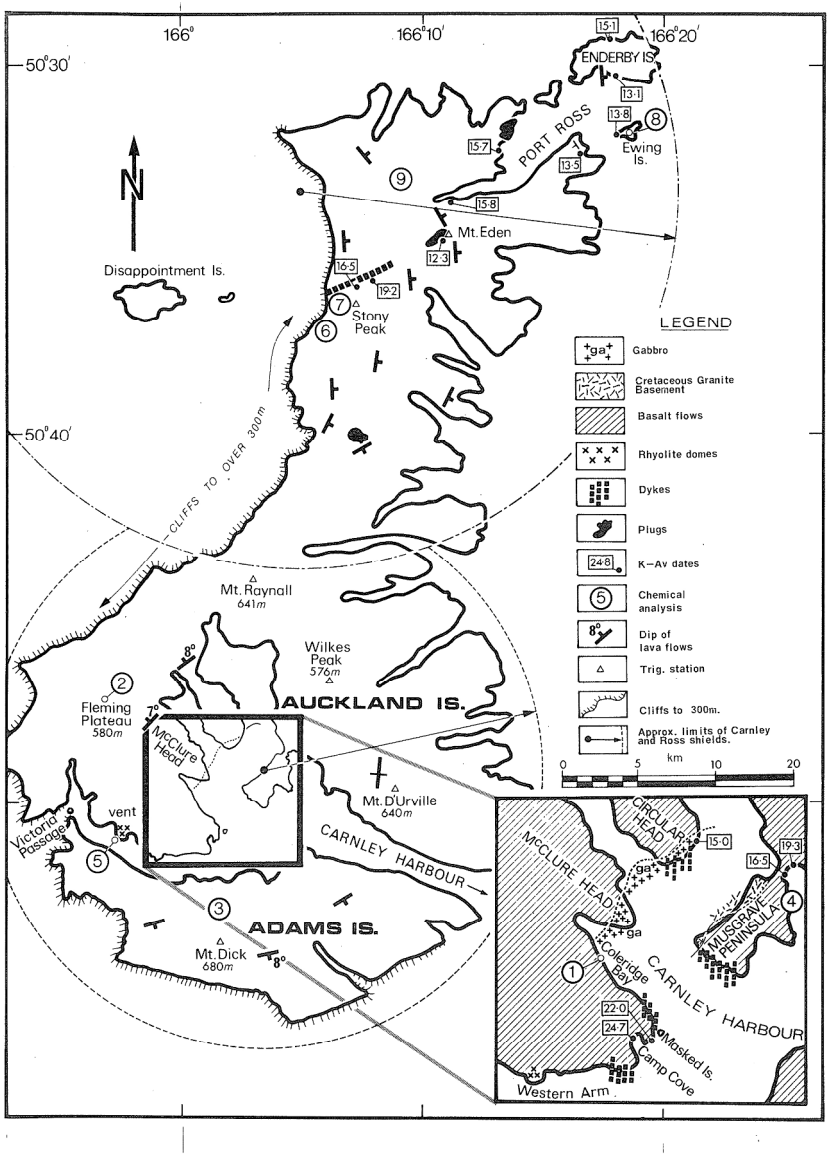

Figure 1 Location map showing Auckland Islands with Carnley Volcano to south and Ross Volcano to north (modified from Gamble and Adams, 1985). The inset map shows the central area of Carnley Harbour, with Cretaceous granite basement on Musgrave Peninsula and a shallow gabbroic intrusion on Circular Head and McClure Head. Dykes of the NNE-SSW trending dyke swarm are stylized. K-Ar age data from Adams, 1983 are in boxes.

210x297mm (300 x 300 DPI)

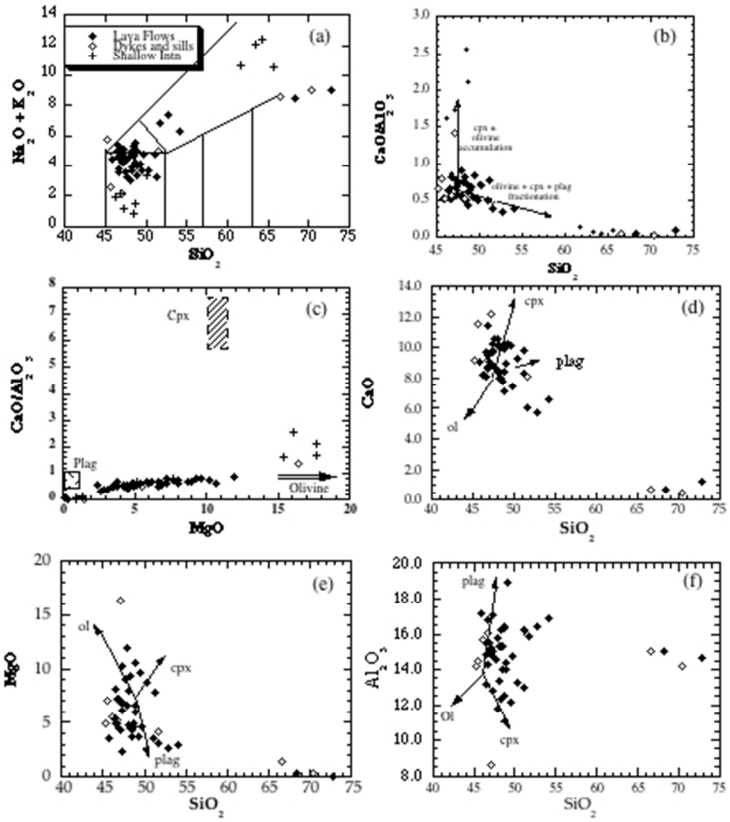

Figure 2 Major oxide variation diagrams (in weight %), including: (a) Total Alkali (Na2O+K2O) v SiO2 (TAS, Le Bas et al, 1986) and (b) MgO v CaO/Al2O3 for lava flows, dikes and sills and shallow intrusions from Auckland Islands. Fractionation vectors are shown for olivine, clinopyroxene and Ca-plagioclase; fractionational crystallisation of a nominated phase produces a trend in the direction of the arrow. Note the strong coherence of the array for mafic rocks and the bimodality between the mafic suite and the felsic samples.

46x61mm (300 x 300 DPI)

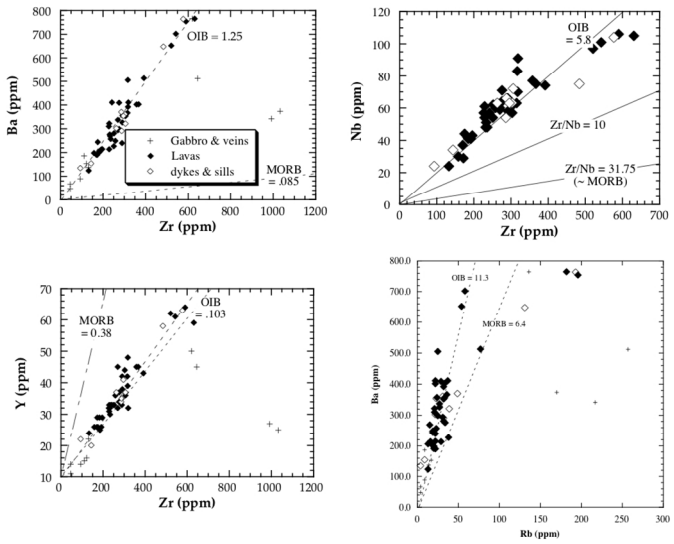

Figure 3 Selected trace element variation diagrams (in parts per million) for Carnley Volcano rocks. OIB and MORB values are from Sun and McDonough, 1989. Note the coherency of highly and moderately incompatible elements Zr, Nb, Y, Ba and Rb in the mafic rocks and the apparent decoupling (crustal assimilation?) in the felsic rocks.

104x148mm (300 x 300 DPI)

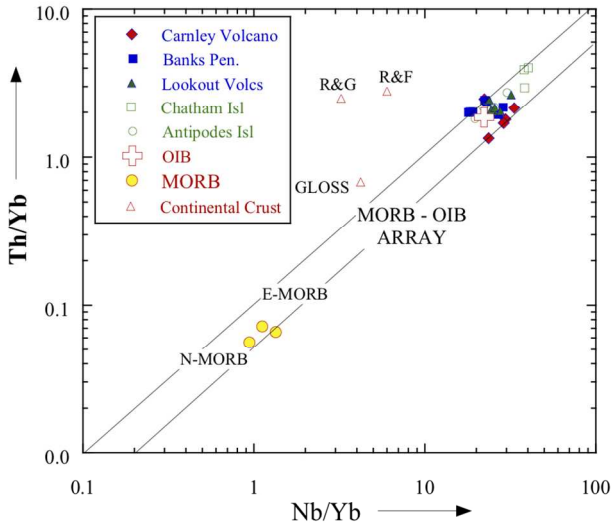

Figure 4 Nb/Yb versus Th/Yb (Pearce, 2008) for intraplate basalts from Auckland Islands, with data from Banks Peninsula (Timm et al., 2010), Lookout Volcanics, Marlborough (McCoy-West et al., 2010), Chatham Islands (Panter et al., 2006) and Antipodes Island (Scott et al., 2013) for comparison. MORB values are from Arevalo and McDonough (2010), continental crust from Rudnick and Gao (R&G) (2003) and Rudnick and Fountain (R&F) (1995), GLOSS from Plank and Langmuir (1989).

104x148mm (300 x 300 DPI)

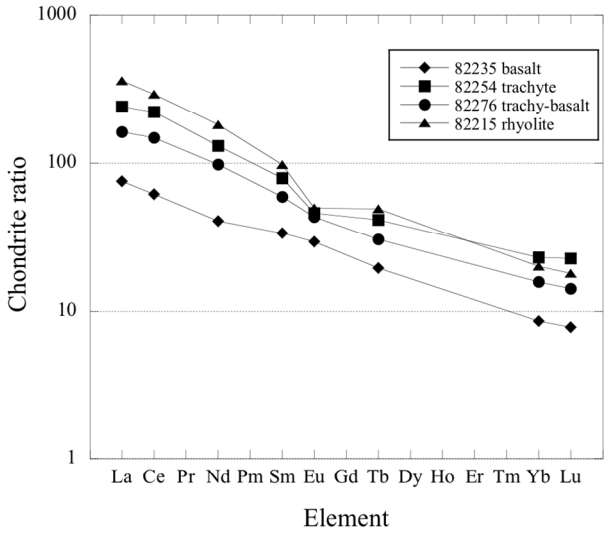

Figure 5 Chondrite normalised (Anders and Gevresse, 1989) Rare Earth Element (REE) diagrams for basalt, trachy-basalt, trachyte and rhyolite from Carnley volcano. Note the enriched LREE patterns and the Eu-anomaly in the trachyte and rhyolite.

104x148mm (300 x 300 DPI)

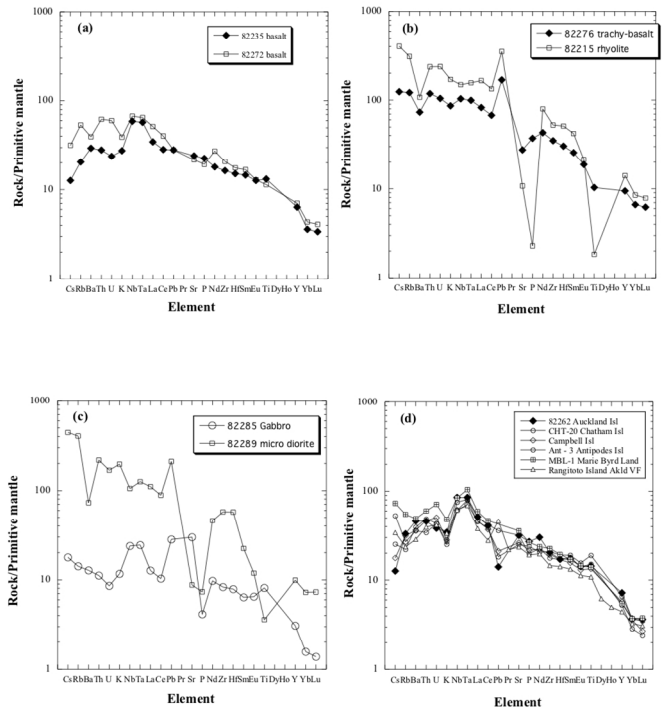

Figure 6 Mantle normalised (Sun and McDonough, 1989) multi-element plots of strongly and moderately incompatible trace elements for selected (a) basalts, (b) evolved rocks and (c) shallow intrusives from the Auckland Islands. Figure 6(d) shows comparative plots for data from Zealandia, West Antarctica, Marie Byrd Land. All the data show a maximum convexity at Nb, Ta and a negative anomaly at K.

104x148mm (300 x 300 DPI)

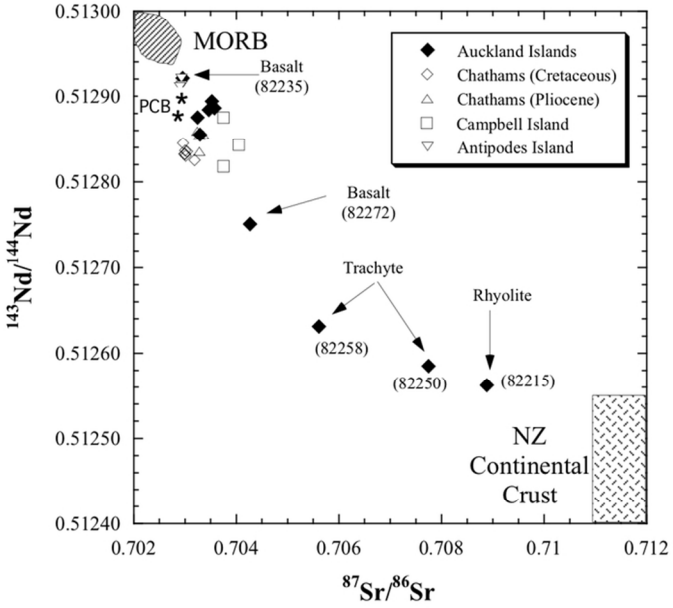

Figure 7 Combined strontium and neodymium isotope variation for the Auckland Islands suite. BSE is bulk silicate earth (Rollinson, 1993). Comparison with data from Chatham Islands, Campbell Island, Antipodes Island and Dunedin volcano (PCB samples), data from Panter et al, 2006; Hoernle et al., 2006 and Price et al, 2003. New Zealand Continental Crust (NZ) is a nominal "average" for quartzo-feldspathic metasediments from compilations by Price et al., 2015, Adams et al., 2005.

74x105mm (300 x 300 DPI)

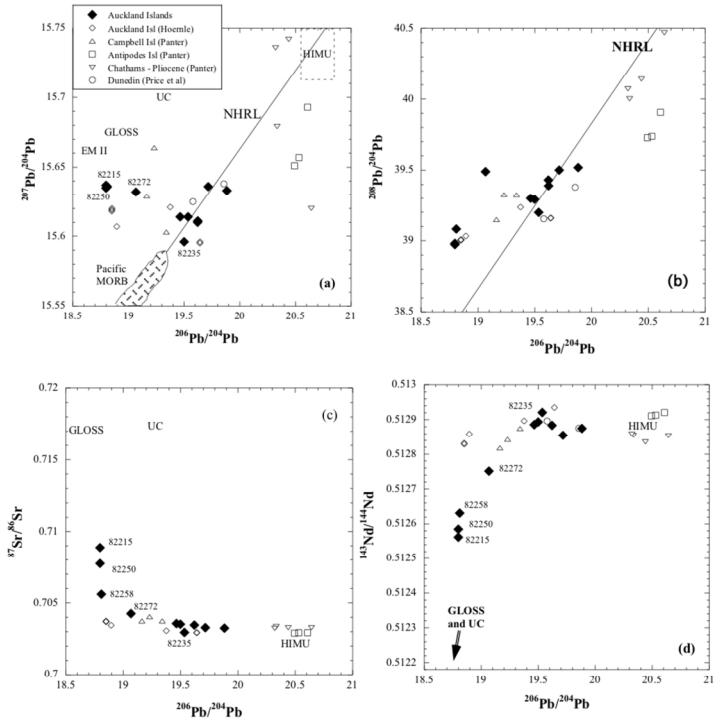

Figure 8 Lead isotope data from Auckland Islands rocks compared with data from other sub Antarctic islands and Dunedin volcano. Evolved trachy-basalt, trachyte and rhyolite samples from Auckland Islands are indicated in Figure 8a, c and d. Nominal averages for continental crust (GLOSS and UC) from Plank and Langmuir (1998) and Rudnick and Gao (2003) are shown. NHRL is the Northern Hemisphere Reference Line (Hart, 1984) HIMU and EM II are mantle reservoirs from Zindler and Hart (1986).

111x157mm (300 x 300 DPI)

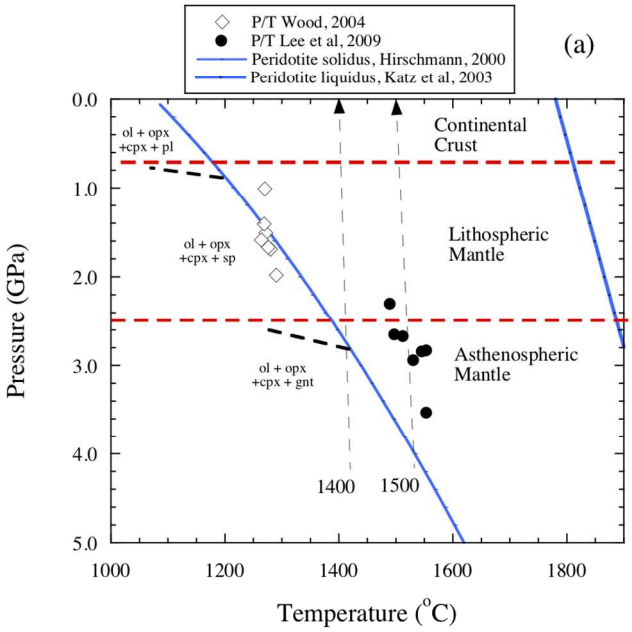

209x297mm (150 x 150 DPI)

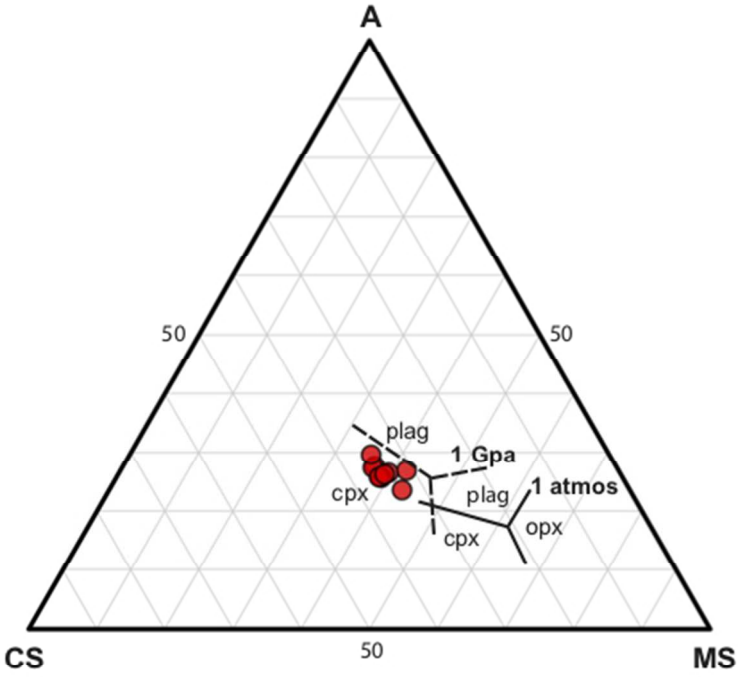

105x86mm (150 x 150 DPI)

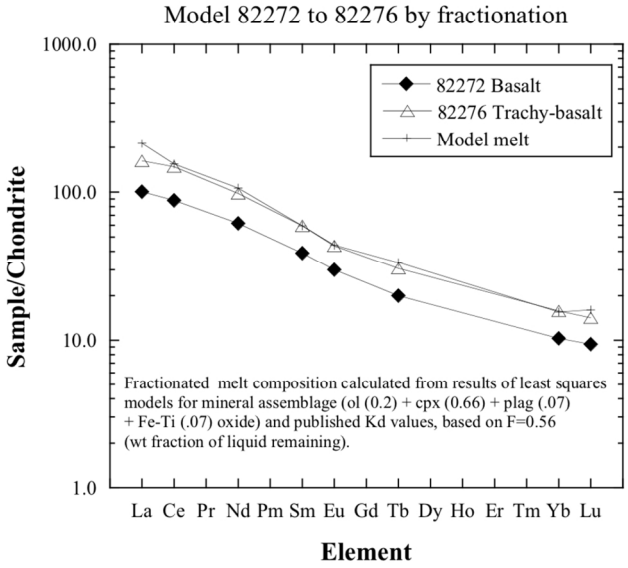

Figure 10. Modelled REE for crystal fractionation calculations, based on results from least squares modelling from basalt (82272) to trachy-basalt (82276).

111x157mm (300 x 300 DPI)

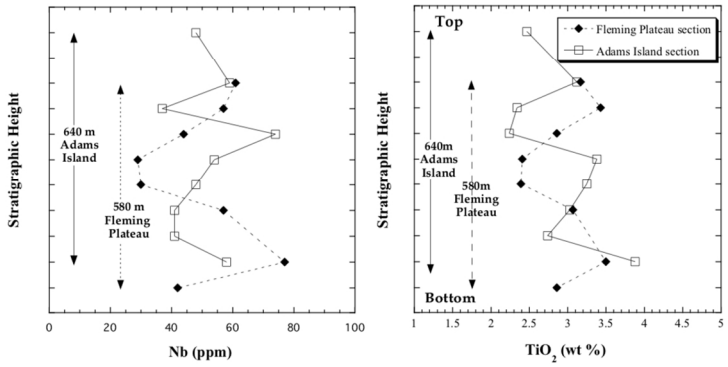

Figure 11 Nb and TiO2 measurements from two measured stratigraphic section of lava flows on Adams Island and the Fleming Plateau (see Fig 1). Note there is no clear chemical variation with height in the section, implying that there is no simple or continuous variation with time.

111x157mm (300 x 300 DPI)

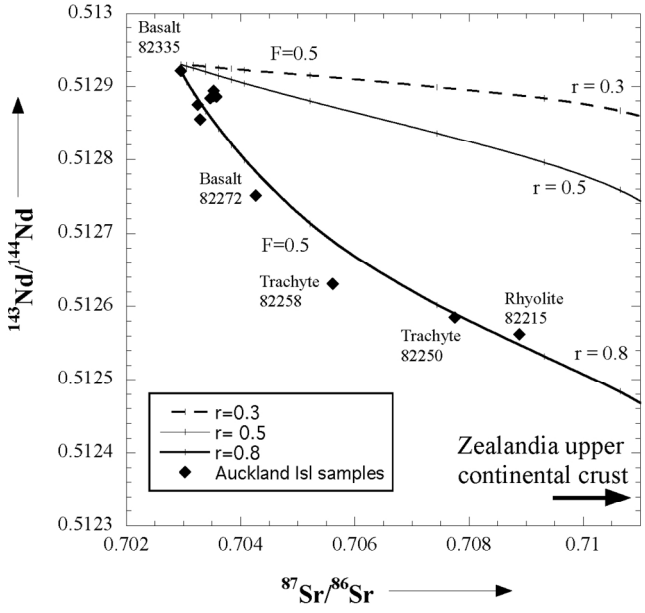

Figure 12 87Sr/86Sr versus 143Nd/144Nd for Auckland Island lavas with calculated AFC curves (De Paolo, 1979) with ticks at 5% intervals, and where r is the ratio of the rate of assimilation to crystallisation.

148x210mm (300 x 300 DPI)

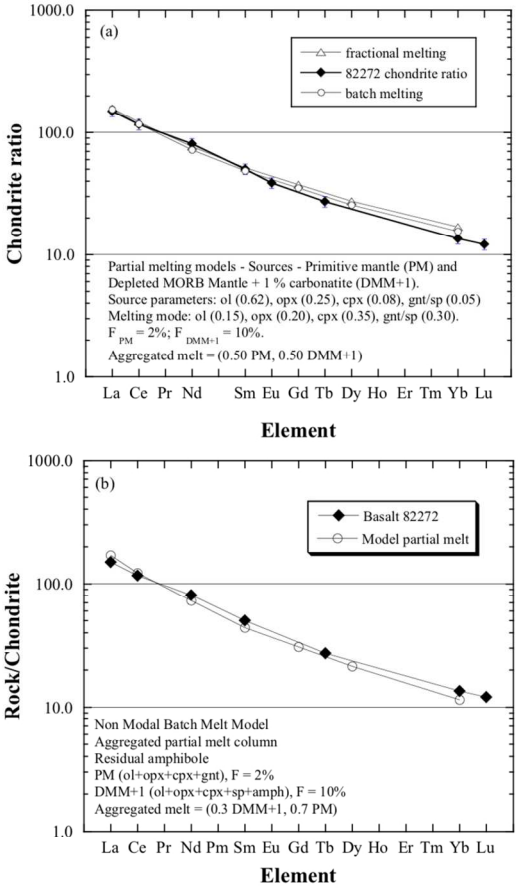

Figure 13 Results of partial melting calculations for basalt (82272) for batch and fractional partial melting, with accumulated aggregated melts. Further details of the partial melting experiments are contained in the diagrams and in Supplementary Materials.

111x157mm (300 x 300 DPI)

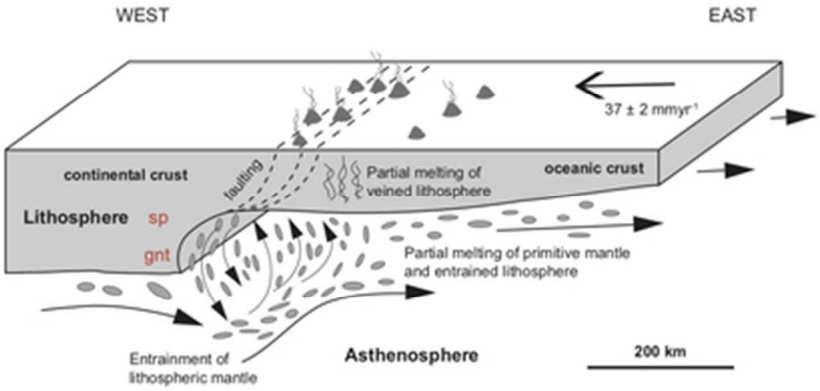

Figure 14. Cartoon cross section of Zealandia lithosphere in the context of "edge driven convection" (after King and Anderson, 1998; Demidjuk et al., 2007 and Price et al., 2014) showing location of intraplate volcanoes and thermo- mechanical erosion (stylised) of base of lithosphere into upwelling asthenospheric mantle leading to magmatism and focusing through deep cross-lithosphere fractures.

35x17mm (300 x 300 DPI)